

Convex Optimization of Linear Impulsive Rendezvous

Boris Benedikter* and Alessandro Zavoli†
Sapienza University of Rome, Rome, 00184, Italy

Nomenclature

a	=	semi-major axis	$\Delta \mathbf{v}$	=	velocity change vector
B	=	actuation matrix	θ	=	true anomaly
e	=	eccentricity	ρ	=	$1 + e \cos \theta$
J	=	objective function	σ	=	free auxiliary variable
k^2	=	h/p^2	Φ	=	state transition matrix
I	=	identity matrix	Ω	=	right ascension of ascending node
i	=	inclination	ω	=	argument of periapsis
h	=	angular momentum	$\ \cdot\ $	=	L^2 norm
M	=	number of grid nodes	Subscripts		
N	=	number of impulses	0	=	initial boundary
\mathbf{r}	=	chaser relative position in the target orbital frame (x, y, z)	f	=	final boundary
p	=	semilatus rectum	Superscripts		
t	=	time	\sim	=	transformed variable
\mathbf{v}	=	chaser relative velocity in the target orbital frame (v_x, v_y, v_z)	\prime	=	derivative with respect to θ
\mathbf{x}	=	state vector	$-$	=	values immediately before an impulse
			$+$	=	values immediately after an impulse

I. Introduction

THIS note aims at providing a concise and self-contained document that describes a clear and easy-to-understand method, that could be useful for a reader that is approaching the linear-impulsive rendezvous topic for the first time, but that is also flexible enough to accommodate problem variations, such as additional constraints like bounded-magnitude $\Delta \mathbf{v}$, or direction constraints with minor modifications.

A convex approach for the optimization of time-fixed non-cooperative rendezvous problems in a linear relative dynamic field is proposed. Despite its simplicity, linear dynamics is very effective to describe the relative motion between two spacecraft (or between one spacecraft and a reference, virtual, satellite), and it is routinely employed in several practical scenarios, such as spacecraft docking [1], proximity operations [2], formation flying [3], collision avoidance [4], and even in unconventional scenarios [5]. Starting with the Clohessy–Wiltshire or Hill equations [6], that are only valid for circular reference orbits, numerous improved versions have been developed in order to account for large-angle gaps [7], elliptic orbit [8, 9], second-order terms [10], and even orbital perturbations [11]. In this note, the Tschauner–Hempel equations [8], valid for reference elliptic orbits of arbitrary eccentricity, are adopted.

*PhD Student, Department of Mechanical and Aerospace Engineering, Sapienza University of Rome, Via Eudossiana 18 - 00184, Rome, Italy; boris.benedikter@uniroma1.it

†Research Assistant, Department of Mechanical and Aerospace Engineering, Sapienza University of Rome, Via Eudossiana 18 - 00184, Rome, Italy; alessandro.zavoli@uniroma1.it

The rendezvous problem, that is, the problem of an active, *chaser*, spacecraft that must reach for a passive, *target*, spacecraft in a given amount of time is a well-known topic in spaceflight mechanics. A number of solution approaches have been developed for both far-field rendezvous, involving a nonlinear two-body dynamics in either passive [12, 13] or cooperative scenarios [14, 15], as well as for the case of the linear dynamics case here investigated. In the latter case, most of the published works focused on the use of the Pontryagin Maximum Principle (PMP) for deriving optimality conditions for propellant-optimal trajectories. The pioneering work of Neustadt [16] states that for linear dynamics in an n -dimensional state-space the optimal transfer requires at most n impulses. By applying the primer vector theory, Lawden derived a set of first-order necessary conditions [17]. Subsequent efforts due to Prussing [18], Carter [19], and Jezewski [20] led to the definition of sufficient conditions for the optimality of a coplanar linear rendezvous problem. Leveraging on these conditions, analytical methods were developed for calculating burn time, magnitude, and direction of the impulsive maneuvers for a fixed number of burns [21, 22]. However, the optimal number of impulses cannot be predicted in advance, and it is usually adjusted iteratively, by inspecting the solution and adding maneuvers or coasting arcs as needed according to PMP [23]. More recently, general closed-form solutions have been derived for linear impulsive rendezvous using accurate dynamics based on relative orbit elements [24].

In this work, the original optimal control problem is transformed into a convex one by discretizing the independent variable over a (sufficiently dense) grid and constraining the impulses to be located at the grid nodes. As a result of the *convexification*, one has a theoretical guarantee of convergence towards the global optimum in a limited, short, time regardless of the initialization. The optimal number of impulses and their epochs (up to some discretization precision) are directly obtained, without the need for any *a priori* assumptions on the solution structure. This is quite a desirable feature of the proposed approach, as the problem finds many applications in time-critical scenarios where both the computational efficiency and the reliability of the algorithm are primary requirements.

This manuscript is organized as follows. Section II describes the original optimal control problem. In Section III, the problem is transcribed into a convex optimization problem. Numerical results are presented in Section IV and compared with those provided by other solution methods. A conclusion section ends the note.

II. Problem Description

A. System Dynamics

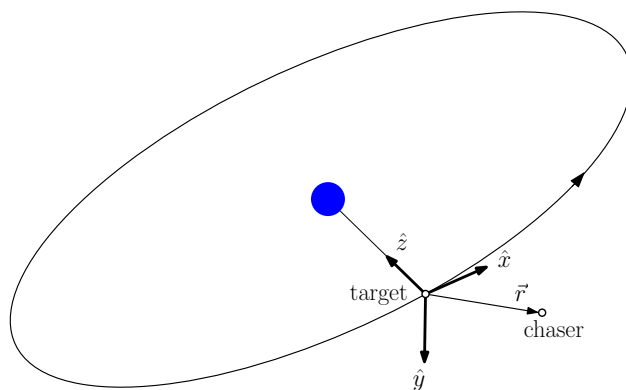


Fig. 1 Orbital Reference frame

This section introduces the Tschauner-Hempel equations that allow describing the linear relative dynamics of a spacecraft with respect to a reference point that moves on a keplerian elliptic orbit of arbitrary eccentricity. The

chaser state \mathbf{x} is completely described by its relative position \mathbf{r} and relative velocity \mathbf{v} with respect to the target, that is, $\mathbf{x} = [\mathbf{r} \quad \mathbf{v}]^T$, that are conveniently expressed in a rotating reference frame, centered in the target spacecraft with the z -axis in the radial direction and pointing towards the Earth and the y -axis in the direction opposite to the angular velocity vector of the target, as shown in Figure 1.

Let $\tilde{\mathbf{x}} = [\tilde{\mathbf{r}} \quad \tilde{\mathbf{v}}]$ be the transformed state, obtained by applying the “direct” transformation:

$$\tilde{\mathbf{r}} = \rho \mathbf{r} \qquad \tilde{\mathbf{v}} = -e \sin \theta \mathbf{r} + 1/(k^2 \rho) \mathbf{v} \quad (1)$$

where e is the eccentricity of the target’s orbit, and ρ and k are defined as

$$\rho = 1 + e \cos \theta \quad (2)$$

$$k^2 = h/p^2 \quad (3)$$

where h and p are the target’s orbit angular momentum and semilatus rectum, respectively. The corresponding inverse transformation is readily available:

$$\mathbf{r} = 1/\rho \tilde{\mathbf{r}} \qquad \mathbf{v} = k^2(e \sin \theta \tilde{\mathbf{r}} + \rho \tilde{\mathbf{v}}) \quad (4)$$

Thanks to the coordinate transformation adopted, the equations of relative motion become:

$$\tilde{x}'' = 2\tilde{z}' \quad (5)$$

$$\tilde{y}'' = -\tilde{y} \quad (6)$$

$$\tilde{z}'' = 3\tilde{z}/\rho - 2\tilde{x}' \quad (7)$$

where $(\)'$ denotes the derivative with respect to the true anomaly θ , which is used as independent variable instead of time t . Please notice that this is a non-autonomous system as ρ depends on the independent variable θ .

Alternatively, the chaser dynamics can be effectively described in terms of the state transition matrix (STM) $\Phi(t_0, t)$ that links the spacecraft transformed state $\tilde{\mathbf{x}}(t)$ at time t , with the transformed state $\tilde{\mathbf{x}}(t_0)$ at time t_0 :

$$\tilde{\mathbf{x}}(\theta) = \Phi(\theta, \theta_0) \tilde{\mathbf{x}}(\theta_0) \quad (8)$$

The STM $\Phi(\theta, \theta_0)$ can be decomposed into STMs for in-plane and out-of-plane motions, respectively. The in-plane relative state at arbitrary θ can be calculated as:

$$\begin{bmatrix} \tilde{x} \\ \tilde{z} \\ \tilde{v}_x \\ \tilde{v}_z \end{bmatrix} = \Phi_\theta \Phi_{\theta_0}^{-1} \begin{bmatrix} \tilde{x}_0 \\ \tilde{z}_0 \\ \tilde{v}_{x_0} \\ \tilde{v}_{z_0} \end{bmatrix} \quad (9)$$

where:

$$\Phi_\theta = \begin{bmatrix} 1 & -c(1+1/\rho) & s(1+1/\rho) & 3\rho^2 J \\ 0 & s & c & 2-3esJ \\ 0 & 2s & 2c-e & 3(1-2esJ) \\ 0 & s' & c' & -3e(s'J+s/\rho^2) \end{bmatrix}_\theta \quad (10)$$

$$\Phi_{\theta_0}^{-1} = \frac{1}{1-e^2} \begin{bmatrix} 1-e^2 & 3es(1/\rho+1/\rho^2) & -es(1+1/\rho) & -ec+2 \\ 0 & -3s(1/\rho+e^2/\rho^2) & s(1+1/\rho) & c-2e \\ 0 & -3(c/\rho+e) & c(1+1/\rho) & -s \\ 0 & 3\rho+e^2-1 & -\rho^2 & es \end{bmatrix}_{\theta_0} \quad (11)$$

and

$$s = \rho \sin \theta \quad (12)$$

$$c = \rho \cos \theta \quad (13)$$

$$s' = \cos \theta + e \cos(2\theta) \quad (14)$$

$$c' = -(\sin \theta + e \sin(2\theta)) \quad (15)$$

$$J = k^2(t - t_0) \quad (16)$$

s' and c' denote the derivatives of s and c with respect to the true anomaly θ . Instead, J is computed using time t , that is related to the true anomaly by Kepler's equation. Finally, the out-of-plane components of the relative state can be computed as:

$$\begin{bmatrix} \tilde{y} \\ \tilde{v}_y \end{bmatrix} = \frac{1}{\rho|\theta-\theta_0|} \begin{bmatrix} c & s \\ -s & c \end{bmatrix}_{\theta-\theta_0} \begin{bmatrix} \tilde{y}_0 \\ \tilde{v}_{y0} \end{bmatrix} \quad (17)$$

B. Optimal Control Problem

An impulsive thrust model is assumed, that is, instantaneous velocity changes $\Delta \mathbf{v}_j = [\Delta v_{x,j} \ \Delta v_{y,j} \ \Delta v_{z,j}]$ are applied at some, unknown, anomalies θ_j , for $j = 1, \dots, N$. By introducing the compact notation $\mathbf{x}_j = \mathbf{x}(\theta_j)$, and using superscripts “-” and “+” to identify the state values immediately before and after the burns, respectively, the general optimization problem can be defined in the compact form:

$$\min_{N, \Delta \tilde{\mathbf{v}}_j, \theta_j} J = \sum_{i=1}^N \Delta v_j \quad (18)$$

$$\text{subject to } \tilde{\mathbf{x}}_1^- = \tilde{\mathbf{x}}_0 \quad (19)$$

$$\tilde{\mathbf{x}}_N^+ = \tilde{\mathbf{x}}_f \quad (20)$$

$$\tilde{\mathbf{x}}_{j+1}^- = \Phi(\theta_{j+1}, \theta_j) \tilde{\mathbf{x}}_j^+ \quad j = 1, \dots, N-1 \quad (21)$$

$$\tilde{\mathbf{x}}_j^+ = \tilde{\mathbf{x}}_j^- + B \Delta \tilde{\mathbf{v}}_j \quad j = 1, \dots, N \quad (22)$$

where $\Delta v = \|\Delta \mathbf{v}\|$ is the magnitude of the velocity change and $B = [0_{3 \times 3} \ I_{3 \times 3}]^T$ is the actuation matrix. Equations (19) and (20) are the initial and terminal conditions, respectively. The initial and final states, $\tilde{\mathbf{x}}_0$ and $\tilde{\mathbf{x}}_f$, are assigned and depend on the specific problem instance. As an example, by enforcing $\tilde{\mathbf{x}}_f = \mathbf{0}$ the rendezvous condition is attained. Nevertheless, this formulation allows for arbitrary terminal conditions and it is also suitable for formation reconfiguration.

Please notice that not only the locations of the velocity impulses are unknown, but also the optimal number of burns N , even though it is constrained in $\mathcal{I} = [1, N_{max}]$, where N_{max} is the cardinality of the state space, that is, 4 in a planar

problem, or 6 in a three-dimensional case, due to Neustadt necessary optimality conditions [16].

III. Convex Formulation

The optimal control problem formulated in Equations (18)–(22) is a general, nonlinear optimization problem since the STM is a nonlinear function of the unknown impulse locations θ_j . Moreover, the problem depends on the optimal number of impulses, which is not known in advance. In general, such a problem might be hard to solve. A common approach consists of fixing N and searching for the location of the impulse, assuming that the first and the last Δv to be applied at the initial and final time, respectively. In particular, N can be set equal to the upper bound N_{max} on the number of impulses. However, optimal solutions of typical problems may require fewer impulses [25], therefore such an approach may not be suitable.

In this work, we propose a numerical method that requires no *a priori* decision on the number of impulses nor on their location. Our approach converts the presented optimal control problem into a Second-Order Cone Programming (SOCP) problem, a special class of convex optimization problems, characterized by a linear objective function, linear equality constraints, and second-order cone constraints. This class of programming problems allows for representing quite complex constraints and can be solved by means of highly-efficient interior point methods, even for a large number of variables [26]. The convexification is carried out by discretizing the problem over a sufficiently dense θ -grid and by constraining the impulses to be located at the grid nodes. In this way, the locations and the total number of impulses are no longer optimization variables, and the corresponding nonlinearities are avoided.

A. Discretization Grid

The independent variable, here the target's true anomaly θ , is discretized into a grid of M points, also referred to as mesh nodes:

$$\theta_0 = \theta_1 < \dots < \theta_M = \theta_f \quad (23)$$

The finite discretization of the independent variable introduces a discretization error on the locations of the impulses, as an instantaneous velocity change can be applied only at those points. State and control variables are discretized over the chosen grid, the differential constraints for each interval can be transformed into algebraic constraints involving the STM:

$$\tilde{\mathbf{x}}_{j+1}^- = \Phi(\theta_{j+1}, \theta_j) \tilde{\mathbf{x}}_j^+ \quad j = 1, \dots, M - 1 \quad (24)$$

Even though the proposed approach poses no restriction on the grid spacing, a uniform node distribution is considered hereafter, as usually one has no prior information on the optimal location of the maneuvers. Intuitively, the quality of the approximation is related to the distance between the nodes and the (true) optimal locations of the impulses: a denser grid will probably allow for a more accurate solution, but will also lead to a more computationally expensive problem. A parametric analysis will be conducted to investigate the effects of the number of discretization points on the overall quality of the attained numerical results.

B. Objective Function

The goal of the optimization is to minimize the overall Δv . Thus, the objective function J can be expressed as the sum of the L^2 norm of the velocity change vectors:

$$J = \sum_{j=1}^M \|\Delta \mathbf{v}_j\|_2 = \sum_{j=1}^M k^2 \rho_j \|\Delta \tilde{\mathbf{v}}_j\|_2 \quad (25)$$

where Eq. (4) has been used to relate the transformed and actual velocity change, and $\rho_j = 1 + e \cos(\theta_j)$ are M known constants, evaluated at the grid nodes.

This formulation provides a convex objective function. However, in a SOCP problem, the objective function must be a linear function of the optimization variables. Hence, we introduce the auxiliary variables σ that represent a free upper bound to the L^2 norm of the velocity change vectors as:

$$\Delta \tilde{v}_{x,j}^2 + \Delta \tilde{v}_{y,j}^2 + \Delta \tilde{v}_{z,j}^2 \leq \sigma_j^2 \quad j = 1, \dots, M \quad (26)$$

Notice that Eq. (26) is a second-order cone constraint, thus suitable for a SOCP formulation. So, in order to minimize the overall Δv , we can equivalently minimize the sum of the newly defined variables:

$$J = \sum_{j=1}^M k^2 \rho_j \sigma_j \quad (27)$$

The resulting SOCP problem is:

$$\min_{\tilde{\mathbf{x}}_j, \Delta \tilde{\mathbf{v}}_j, \sigma_j} J = \sum_{j=1}^M k^2 \rho_j \sigma_j \quad (28)$$

$$\text{subject to } \tilde{\mathbf{x}}_1^- = \tilde{\mathbf{x}}_0 \quad (29)$$

$$\tilde{\mathbf{x}}_M^+ = \tilde{\mathbf{x}}_f \quad (30)$$

$$\tilde{\mathbf{x}}_{j+1}^- = \Phi(\theta_{j+1}, \theta_j) \tilde{\mathbf{x}}_j^+ \quad j = 1, \dots, M-1 \quad (31)$$

$$\Delta \tilde{v}_{x,j}^2 + \Delta \tilde{v}_{y,j}^2 + \Delta \tilde{v}_{z,j}^2 \leq \sigma_j^2 \quad j = 1, \dots, M \quad (32)$$

$$\tilde{\mathbf{x}}_j^+ = \tilde{\mathbf{x}}_j^- + B \Delta \tilde{\mathbf{v}}_j \quad j = 1, \dots, M \quad (33)$$

IV. Numerical Results

In order to demonstrate the effectiveness of the proposed approach, three test cases, whose optimal solution is available in literature, are here considered: i) a four-impulse rendezvous with a target in a circular orbit, ii) a three-impulse approach maneuver for the Automated Transfer Vehicle (ATV) to the International Space Station, and iii) a reconfiguration of a spacecraft formation flying on a highly elliptic orbit for the SIMBOL-X mission. For the sake of simplicity, only the in-plane motion is shown here, as in-plane and out-plane motions are decoupled in the considered dynamical model. Hereafter, the state variables y and v_y are thus dropped. Numerical results are provided for a uniform mesh with $M = 257$ nodes. The effect of the mesh size on the quality of the attained solutions is then discussed.

A. Circle-to-Circle Rendezvous

Let us consider a chaser spacecraft flying on a circular orbit of radius r_0 that has to rendezvous with a target on a circular orbit of radius $r_f = 1.2r_0$. In particular, by setting the target orbit radius r_f and mean motion equal to one, the problem boundary conditions are $\mathbf{r}_0 = [-\pi \ 0 \ 1/6]$, $\mathbf{v}_0 = [1/4 \ 0 \ 0]$, $\mathbf{r}_f = [0 \ 0 \ 0]$, and $\mathbf{v}_f = [0 \ 0 \ 0]$, respectively. The mission must be accomplished in a limited time, corresponding to $\theta_f = 10$ rad.

Table 1 Results for the four-impulse rendezvous

Parameter	Convex	Optimal
θ_1 (rad)	0	0
θ_2 (rad)	2.8125	2.8033
θ_3 (rad)	7.1875	7.1967
θ_4 (rad)	10.0000	10.0000
$\Delta\mathbf{v}_1$	$\begin{bmatrix} -0.01596 & +0.00421 \end{bmatrix}$	$\begin{bmatrix} -0.01575 & +0.00415 \end{bmatrix}$
$\Delta\mathbf{v}_2$	$\begin{bmatrix} -0.02989 & +0.00162 \end{bmatrix}$	$\begin{bmatrix} -0.03028 & +0.00158 \end{bmatrix}$
$\Delta\mathbf{v}_3$	$\begin{bmatrix} +0.06309 & +0.00343 \end{bmatrix}$	$\begin{bmatrix} +0.06387 & +0.00333 \end{bmatrix}$
$\Delta\mathbf{v}_4$	$\begin{bmatrix} +0.06553 & +0.01719 \end{bmatrix}$	$\begin{bmatrix} +0.06549 & +0.01724 \end{bmatrix}$
Overall Δv	0.17828	0.17828

Table 1 compares the solution found by the present procedure with the optimal one, obtained by using an indirect technique that the authors routinely applied in the past for solving optimal control problems [27–29]. The convex approach succeeds in capturing the optimal 4-impulse structure of the mission, with one impulse at the departure, one at the arrival, and two burns at intermediate maneuvering points. Besides these four points, the magnitude of the velocity changes σ_j over the mesh points is several orders of magnitude lower than the actual impulses. The two solutions are in good agreement. The overall Δv is evaluated accurately. Minor differences arise in the locations of the intermediate impulses, which are captured at the grid points that are closer to the optimal locations found by the indirect method (as the adopted grid made up of 257 equally spaced nodes does not include the optimal θ_2 and θ_3). The shift of the intermediate impulses induces minimal changes in each $\Delta\mathbf{v}$ vector which, in turns, cause negligible changes in the overall trajectory (see Fig. 2).

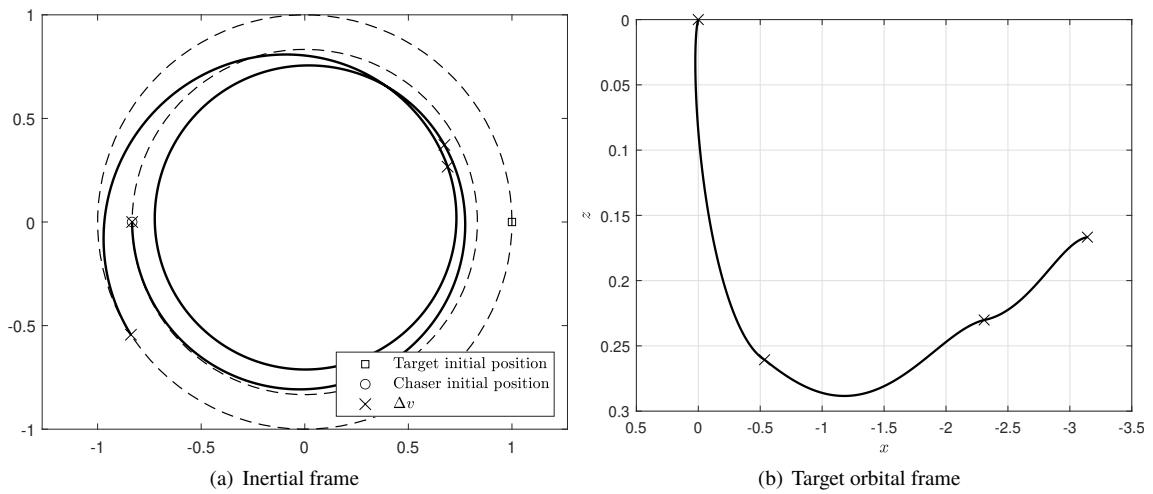


Fig. 2 Four-impulse trajectory

B. ATV Approaching Maneuver

The second case study concerns a more practical scenario, where the Automated Transfer Vehicle (ATV) needs to approach the International Space Station [30]. An example is discussed by Louembet [31], where the optimal trajectory to move the ATV from about 30 km to 100 m to the ISS is investigated. More precisely, the following initial conditions $\mathbf{r}_0 = [-30 \ 0 \ 0.5]$ km, $\mathbf{v}_0 = [8.514 \ 0 \ 0]$ m/s, and final conditions $\mathbf{r}_f = [-0.1 \ 0 \ 0]$ km, $\mathbf{v}_f = [0 \ 0 \ 0]$ m/s are prescribed. The orbital elements of the target orbit and the transfer duration Δt are reported in Table 2.

Table 2 Data for the ATV rendezvous

Parameter	Value
a (km)	6763.00
e	0.0052
i (deg)	52.00
Ω (deg)	0.00
ω (deg)	0.00
θ_0 (deg)	0.00
Δt (s)	55 350

Table 3 Results for the ATV mission

Parameter	Convex ($M = 257$)	Convex ($M^* = 3$)	Optimal
θ_1 (rad)	0	0	0
θ_2 (rad)	59.88620	59.90800	59.89691
θ_3 (rad)	60.13170		
θ_4 (rad)	62.83150	62.83150	62.83149
$\Delta \mathbf{v}_1$ (m/s)	$\begin{bmatrix} -7.55410 & +0.23649 \end{bmatrix}$	$\begin{bmatrix} -7.55410 & +0.23952 \end{bmatrix}$	$\begin{bmatrix} -7.55410 & +0.23877 \end{bmatrix}$
$\Delta \mathbf{v}_2$ (m/s)	$\begin{bmatrix} +0.13839 & +0.00141 \end{bmatrix}$	$\begin{bmatrix} +0.14439 & +0.00085 \end{bmatrix}$	$\begin{bmatrix} +0.14422 & +0.00086 \end{bmatrix}$
$\Delta \mathbf{v}_3$ (m/s)	$\begin{bmatrix} +0.00564 & +0.00003 \end{bmatrix}$		
$\Delta \mathbf{v}_4$ (m/s)	$\begin{bmatrix} +0.04138 & +0.00126 \end{bmatrix}$	$\begin{bmatrix} +0.04125 & +0.00131 \end{bmatrix}$	$\begin{bmatrix} +0.04147 & +0.00130 \end{bmatrix}$
Overall Δv (m/s)	7.74357	7.74356	7.74356

The optimal solution and the one attained for a 257-node grid are reported in Table 3. The optimal transfer found out by Louembet [31], is made up of three impulses: one at the departure, one at the arrival, and one at an intermediate point. This problem is numerically more challenging than the previous one, as the optimal solution presents two burns much smaller than the initial one, and the change in the transversal direction is of about three orders of magnitude. Indeed, the convex approach shows some difficulties in determining precisely the exact location of the intermediate maneuver. Rather, the intermediate impulse is spread over adjacent nodes. Eventually, a "sub-optimal" four-impulse solution is detected: the 2nd impulse is close to the optimal one, the 3rd impulse is much lower but it is retained, because greater than the allowed tolerance 10^{-5} . However, the difference in the overall mission cost is about 10^{-5} , which is close to the optimization tolerance.

For the sake of completeness, a parametric investigation has been carried out, by considering a 3-nodes grid and moving the inner node location over the domain. A clear minimum is identified and the best-found solution (named $M^* = 3$) is also reported in Table 3.

C. SIMBOL-X

Finally, let us consider a case where the reference orbit is highly elliptical, as in the case of the SIMBOL-X mission [32]. An approach maneuver from 30 km to 500 m from the target is investigated. Specifically, the initial conditions $\mathbf{r}_0 =$

$[18.3095 \ 0 \ -23.7647]$ km, $\mathbf{v}_0 = [-0.0542 \ 0 \ -0.0418]$ m/s, and final conditions $\mathbf{r}_f = [335.12 \ 0 \ -371.1]$ m, $\mathbf{v}_f = [0.00155 \ 0 \ 0.0014]$ m/s are prescribed. Table 4 reports the target orbital elements and the duration of the maneuver.

Table 4 Data for the SIMBOL-X rendezvous

Parameter	Value
a (km)	106 246.98
e	0.7988
i (deg)	5.20
Ω (deg)	90.00
ω (deg)	180.00
θ_0 (deg)	135.00
Δt (s)	49 995

Table 5 Results for the SIMBOL-X mission

Parameter	Convex	Optimal
θ_1	2.3562	2.3562
θ_2	2.7859	2.7859
$\Delta \mathbf{v}_1$ (m/s)	$\begin{bmatrix} -0.6193 & +0.5061 \end{bmatrix}$	$\begin{bmatrix} -0.6193 & +0.5061 \end{bmatrix}$
$\Delta \mathbf{v}_2$ (m/s)	$\begin{bmatrix} +0.1748 & -0.4912 \end{bmatrix}$	$\begin{bmatrix} +0.1748 & -0.4912 \end{bmatrix}$
Overall Δv (m/s)	1.3212	1.3212

The final solution is a two-impulse transfer, as reported in Table 5. The solution attained with the convex approach is identical to the optimal one, provided by Arzelier et al. [33]. Indeed, in this case, the impulses are located at the initial and final time, respectively, which belong to the mesh grid; hence, the impulses are captured at their exact optimal location.

D. Effects of the Mesh Grid

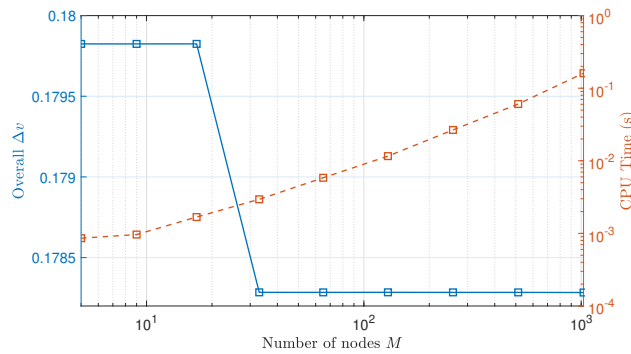


Fig. 3 Four-impulse overall Δv and computation time as a function of the number of discretization nodes for the circle-to-circle example

A parametric study on the effects of the mesh size has also been carried out, in order to investigate its role on the solution quality in terms of overall Δv estimation, computational time, and accuracy on the location of the maneuvering points. Intuitively, one expects that, as the mesh density increases, the distance between the optimal locations of the internal impulses and the (closest) grid nodes decreases, leading to a numerical solution closer to the optimal one.

Figure 3 shows the overall mission cost for the circle-to-circle rendezvous mission, and the corresponding computational time, as a function of the number of grid points. The overall Δv quickly converges towards the optimal value. Instead, the computational cost increases almost linearly in the number of nodes. The use of a mesh grid with a small, limited, number of nodes seems thus justified. It is also worth mentioning that the computation time is quite short even for the largest attempted grid because the convex formulation allows for the use of highly-efficient algorithms.

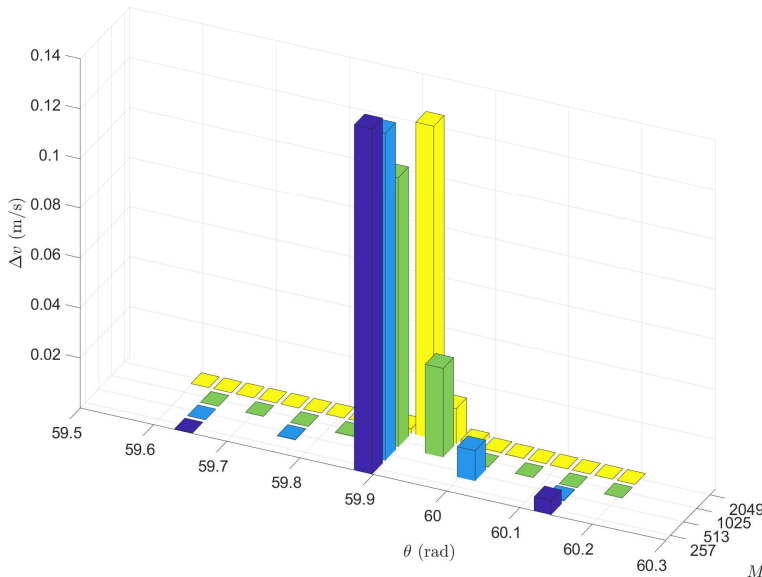


Fig. 4 Distribution of the Δv magnitudes for different mesh sizes in the neighborhood of the intermediate impulse in the ATV test case.

On the other hand, increasing the number of grid points may lead to numerical issues related to the accumulation of truncation and round-off errors. Due to the finite precision (i.e., tolerance) of the optimization process, in some circumstances, an impulse may be spread over a set of neighboring nodes. An example is proposed in Figure 4, where the distribution of the velocity change magnitudes in the neighborhood of the (optimal) intermediate impulse location for the ATV test case is presented. Even though this issue could be mitigated by tightening the optimization tolerances and by selecting a suitable set of nondimensionalization factors to properly scale the problem, the current analysis does not provide a systematic way to avoid this problem, which manifests when too many grid nodes are located in the proximity of the optimal maneuvering point.

V. Conclusion

This note presented a convex formulation of the time-fixed optimal rendezvous in a linear dynamics. The Tschauner-Hempel equations are used to describe the motion of the chaser spacecraft relative to a target that flies on a keplerian orbit of arbitrary eccentricity. The original non-convex problem is transformed into a convex one by using a gridding technique, that is, by introducing a finite discretization of the independent variable domain: impulse locations are constrained to the grid nodes, and the differential constraints are replaced by algebraic constraints involving the state transition matrix between adjacent nodes. The convex formulation allows the use of special solution algorithms that guarantee the convergence towards the global optimum within a limited computation time, even when a large number of

variables are involved, and that does not require any sort of initialization.

Numerical results show a good agreement between the convex solution and the optimal one, provided by other approaches. In cases of practical interest, a limited number of nodes is sufficient to get an accurate solution in terms of both trajectory and mission cost. A parametric study on the effects of the mesh size discourages the use of very-fine grids. In fact, the accumulation of truncation errors and the finite precision of the adopted convex solver may hinder the effectiveness of the approach. Instead, the use of medium-to-coarse grids allows to get the most out of this approach: the overall Δv cost quickly converges towards the optimal value, and the computational effort is kept to the minimum. These features make the proposed approach suitable for time-critical applications, such as autonomous guidance, and other computationally demanding tasks.

References

- [1] Weiss, A., Baldwin, M., Erwin, R. S., and Kolmanovsky, I., "Model predictive control for spacecraft rendezvous and docking: Strategies for handling constraints and case studies," *IEEE Transactions on Control Systems Technology*, Vol. 23, No. 4, 2015, pp. 1638–1647.
- [2] Subbarao, K., and Welsh, S. J., "Nonlinear control of motion synchronization for satellite proximity operations," *Journal of guidance, control, and dynamics*, Vol. 31, No. 5, 2008, pp. 1284–1294.
- [3] Vassar, R. H., and Sherwood, R. B., "Formationkeeping for a Pair of Satellites in a Circular Orbit," *Journal of Guidance, Control, and Dynamics*, Vol. 8, No. 2, 1985, pp. 235–242.
- [4] Epenoy, R., "Fuel-optimal trajectories for continuous-thrust orbital rendezvous with collision avoidance constraint," *Advances in the Astronautical Sciences*, Vol. 140, No. 2, 2011, pp. 341–360.
- [5] Zavoli, A., Federici, L., Benedikter, B., Casalino, L., and Colasurdo, G., "GTOC X: Solution Approach of Team Sapienza-PoliTo," *Paper AAS 19-894, Astrodynamics Specialist Conference*, Portland, Maine, 2019.
- [6] Hill, G. W., "Researches in the lunar theory," *American journal of Mathematics*, Vol. 1, No. 1, 1878, pp. 5–26.
- [7] Baranov, A., "An algorithm for calculating parameters of multi-orbit maneuvers in remote guidance," *Cosmic Research*, Vol. 28, No. 1, 1990, pp. 61–67.
- [8] Tschauner, J., and Hempel, P., "Rendezvous zu einem in elliptischer Bahn umlaufenden Ziel," *Astronautica Acta*, Vol. 11, No. 2, 1965, pp. 104–+.
- [9] Yamanaka, K., and Ankersen, F., "New State Transition Matrix for Relative Motion on an Arbitrary Elliptical Orbit," *Journal of Guidance, Control, and Dynamics*, Vol. 25, No. 1, 2002, pp. 60–66. <https://doi.org/10.2514/2.4875>.
- [10] Kechichian, J., "Techniques of accurate analytic terminal rendezvous in near-circular orbit," *Acta Astronautica*, Vol. 26, No. 6, 1992, pp. 377–394. [https://doi.org/10.1016/0094-5765\(92\)90068-t](https://doi.org/10.1016/0094-5765(92)90068-t).
- [11] Schweighart, S. A., and Sedwick, R. J., "High-Fidelity Linearized J Model for Satellite Formation Flight," *Journal of Guidance, Control, and Dynamics*, Vol. 25, No. 6, 2002, pp. 1073–1080. <https://doi.org/10.2514/2.4986>.
- [12] Mirfakhraie, K., and Conway, B. A., "Optimal cooperative time-fixed impulsive rendezvous," *Journal of Guidance Control Dynamics*, Vol. 17, 1994, pp. 607–613. <https://doi.org/10.2514/3.21240>.
- [13] Lu, P., and Liu, X., "Autonomous trajectory planning for rendezvous and proximity operations by conic optimization," *Journal of Guidance, Control, and Dynamics*, Vol. 36, No. 2, 2013, pp. 375–389.

- [14] Benedikter, B., Zavoli, A., and Colasurdo, G., “A Convex Optimization Approach for Finite-Thrust Time-Constrained Cooperative Rendezvous,” *Paper AAS 19-763, Astrodynamics Specialist Conference*, Portland, Maine, 2019.
- [15] Zavoli, A., and Colasurdo, G., “Indirect optimization of finite-thrust cooperative rendezvous,” *Journal of Guidance, Control, and Dynamics*, Vol. 38, No. 2, 2015, pp. 304–314. <https://doi.org/10.2514/1.G000531>, cited By 6.
- [16] Neustadt, L. W., “Optimization, a moment problem, and nonlinear programming,” *Journal of the Society for Industrial and Applied Mathematics, Series A: Control*, Vol. 2, No. 1, 1964, pp. 33–53.
- [17] Lawden, D., “General theory of optimal rocket trajectories,” *Optimal trajectories for space navigation*, 1963, pp. 54–78.
- [18] Prussing, J. E., “Optimal impulsive linear systems- Sufficient conditions and maximum number of impulses,” *Spaceflight mechanics 1994*, 1994, pp. 1015–1023.
- [19] Carter, T., “Optimal impulsive space trajectories based on linear equations,” *Journal of optimization theory and applications*, Vol. 70, No. 2, 1991, pp. 277–297.
- [20] Jezewski, D., “Primer vector theory applied to the linear relative-motion equations,” *Optimal Control Applications and Methods*, Vol. 1, No. 4, 1980, pp. 387–401. <https://doi.org/10.1002/oca.4660010408>.
- [21] Prussing, J., “Optimal four-impulse fixed-time rendezvous in the vicinity of a circular orbit.” *AIAA Journal*, Vol. 7, No. 5, 1969, pp. 928–935.
- [22] Carter, T. E., and Alvarez, S. A., “Quadratic-based computation of four-impulse optimal rendezvous near circular orbit,” *Journal of Guidance, Control, and Dynamics*, Vol. 23, No. 1, 2000, pp. 109–117.
- [23] LION, P. M., and HANDELSMAN, M., “Primer vector on fixed-time impulsive trajectories.” *AIAA Journal*, Vol. 6, No. 1, 1968, pp. 127–132. <https://doi.org/10.2514/3.4452>.
- [24] Chernick, M., and D’Amico, S., “New closed-form solutions for optimal impulsive control of spacecraft relative motion,” *Journal of Guidance, Control, and Dynamics*, Vol. 41, No. 2, 2017, pp. 301–319.
- [25] Prussing, J. E., “Optimal two-and three-impulse fixed-time rendezvous in the vicinity of a circular orbit,” *Journal of Spacecraft and Rockets*, Vol. 40, No. 6, 2003, pp. 952–959.
- [26] Alizadeh, F., and Goldfarb, D., “Second-order cone programming,” *Mathematical programming*, Vol. 95, No. 1, 2003, pp. 3–51.
- [27] Colasurdo, G., and Pastrone, D., “Indirect optimization method for impulsive transfers,” *Astrodynamics Conference*, American Institute of Aeronautics and Astronautics, 1994. <https://doi.org/10.2514/6.1994-3762>.
- [28] Zavoli, A., Simeoni, F., Casalino, L., and Colasurdo, G., “Optimal cooperative deployment of a two-satellite formation into a highly elliptic orbit,” *Advances in the Astronautical Sciences*, Vol. 142, 2012, pp. 3647–3663.
- [29] Simeoni, F., Casalino, L., Zavoli, A., and Colasurdo, G., “Indirect optimization of satellite deployment into a highly elliptic orbit,” *International Journal of Aerospace Engineering*, Vol. 2012, 2012, p. 14. <https://doi.org/10.1155/2012/152683>.
- [30] Amadiou, P., and Heloret, J., “The automated transfer vehicle,” *Air and Space Europe*, Vol. 1, No. 1, 1999, pp. 76 – 80. [https://doi.org/https://doi.org/10.1016/S1290-0958\(99\)80044-6](https://doi.org/https://doi.org/10.1016/S1290-0958(99)80044-6), URL <http://www.sciencedirect.com/science/article/pii/S1290095899800446>.
- [31] Louembet, C., “Contributions au guidage pour le rendez-vous spatial par résolution du problème de commande optimale impulsione,” Ph.D. thesis, Université Toulouse 3 Paul Sabatier (UT3 Paul Sabatier), 2017.

- [32] Gaudel, A., Berges, J.-C., Trapier, T., Gamet, P., and Djalal, S., “Autonomous rendezvous guidance function of the SIMBOL-X formation flying mission a high elliptical orbit: Preliminary design and performance analysis,” *Proceedings of the 21st International Symposium on Space Flight Dynamics*, 2010.
- [33] Arzelier, D., Kara-Zaitri, M., Louembet, C., and Delibasi, A., “Using polynomial optimization to solve the fuel-optimal linear impulsive rendezvous problem,” *Journal of Guidance, Control, and Dynamics*, Vol. 34, No. 5, 2011, pp. 1567–1576.